CHEMISTRY
A EUROPEAN JOURNAL

DOI: 10.1002/chem.200903133

Designed Smart System of the Sandwiched and Concentric Architecture of $RuO_2/C/RuO_2$ for High Performance in Electrochemical Energy Storage

Yu Wang,*[a] Ce Yao Foo,[a, b] Tun Kai Hoo,[a, c] Mark Ng,[a] and Jianyi Lin*[a]

Energy has been an important topic since the extraction and consumption of fossil energy from nature became the major means to improve our quality of life.[1–5] However, crude oil and charcoal stored underneath the earth millions or even billions of years ago are becoming less available, and the greenhouse effect is becoming more serious and endangering the global environment derived from combustion of gasoline and other hydrocarbons. Hence, people have come to realize that the only way for us to maintain sustainable development is to harvest even more energy from the sun than ever and to change our current lifestyles that are dependent on the large-scale consumption of natural resources. As a result, more and more efforts have been made to find ways to utilize renewable energy from the sun or wind, or from nuclear energy efficiently.[2,3] Generally all of the above-mentioned resources have to be converted into electrical energy prior to their application with the exception of direct heating. Accordingly, the development of electrical-energy storage techniques (commonly referred as batteries), especially Li-ion batteries and other rechargeable devices such as electrochemical capacitors (ECs), has definitely become more urgent.[6–9] Effective utilization of electricity cannot only substantially support the strategy of sustainable development, but also reduce CO_2 or other greenhouse gas emissions in an attempt to relieve the increasing pressure from global warming significantly. However, among all of the means to store electrical energy, ECs (also known as supercapacitors or ultracapacitors) have attracted less attention than the Li-ion battery until very recently. Li-ion batteries encounter a big problem when faster power delivery or uptake is required, for example, in some practical fields such as electric vehicles and other large industrial equipments.[10] ECs have the unique advantage of full and rapid charge–discharge within a few seconds and a much higher power density ($10\,kW\,kg^{-1}$) than the Li-ion battery, and can potentially be complementary or even replace batteries in some uninterruptible systems to serve as back-up power supplies and protect devices from damage as a consequence of power disruption.[11] On the basis of earlier work, it has been concluded that at least three types of ECs have been developed up to now, and two distinct mechanisms of electrochemical energy storage have been detected. These include electrochemical double-layer capacitors (EDLCs), pseudocapacitors, and hybrid capacitors, which jointly consist of the above two capacitors and can definitely benefit from the combined properties of capacitive and faradic capacitance.[2,12] EDLCs are designed based on the discovery by Helmholtz in 1853,[2] and the capacitive behavior is restricted from 5 to $20\,\mu F cm^{-2}$.[13] So even though the specific surface area of the active material could reach up to $1000\,m^2\,g^{-1}$ and new findings of capacitive performance in small pores have been uncovered,[14] the specific capacitances cannot exceed $200\,F\,g^{-1}$. Nevertheless, the low production cost of this kind of capacitor has resulted in their current wide use.[8] The second type of supercapacitor was developed from the intrinsic reversibility of redox couples dispersed on the surface or near-surface areas of the electroactive material.[15–17] Ultrahigh pseudocapacitance is the most fascinating characteristic of such capacitors; however, the typical electrode materials of pseudocapacitors, including conducting polymers and transition-metal oxides, are either more expensive or exhibit poorer conductivity compared with activated carbon used in EDLCs, which make them not ideal for supercapacitors of the next generation.[18] Thus, the latest type of ECs have been exploited and a great deal of

[a] Dr. Y. Wang, C. Y. Foo, T. K. Hoo, M. Ng, Prof. J. Lin
Institute of Chemical and Engineering Sciences
1, Pesek Road, Jurong Island, Singapore, 627833
Fax: (65) 63166185
E-mail: wang_yu@ices.a-star.edu.sg
lin_jianyi@ices.a-star.edu.sg

[b] C. Y. Foo
School of Materials Science and Engineering
Nanyang Technological University
Nanyang Avenue, Singapore 639798

[c] T. K. Hoo
School of Chemical and Biomedical Engineering
Nanyang Technological University
62 Nanyang Drive, Singapore, 637459

Supporting information for this article is available on the WWW under http://dx.doi.org/10.1002/chem.200903133.

enthusiasm has gone into this relatively new field because of its underlying ability to conquer the drawbacks existing in the former two types of capacitors.

From a general point of view, mesoporous, 3D, regular/aperiodic architectures are desirable for the penetration or diffusion of an electrolyte into the innermost layers of electrode materials so that the electrolyte can totally saturate the accessible surface areas of the matrix and greatly enhance the specific capacitance. Meanwhile, excellent electronic conductivity together with rapid ionic transportation and exchange occurring on the interface between the electrode materials and the electrolyte are other prerequisite conditions to promote the electrochemical performance in charge storage. With these factors in mind, a number of achievements have been made in which composite structures consisting of activated carbon grain, arrayed carbon nanotubes (CNT), and carbon rods decorated with pseudocapacitive materials[19–21] or pure functional electrode materials with nanotubular and porous film-shaped morphologies[18] have been highlighted. However, in most of these cases either too high loading of the pseudocapacitive materials or low efficiency of electrolyte penetration and low utilization of the surface area has occurred. To make good use of all of the exposed surfaces including the outer and inner surface areas and to lower the loading ratio of the pseudoactive materials to activated carbon, more advanced and smarter systems have to be designed that are aimed at charge storage applications. However, this still remains a great challenge for us and deserves to be paid more attention.

Herein, we report a facile and versatile method to synthesize one kind of novel sandwiched architecture that exhibits a hollow nanosphere and a concentric shell consisting of three-fold layers of RuO_2/C/RuO_2. This product has a high surface area and a well-graphitized mesoporous carbon shell. Upon precisely controlling the amount of pseudocapacitive material added into the precursors, the loading ratio of hydrous metal oxides, especially $RuO_2{\cdot}xH_2O$, can be limited below 15% with respect to the total mass, hence the preparation cost will be significantly reduced. Owing to the hollow nature of the product, both the outer and inner surface areas could be completely utilized. The most promising pseudocapacitive materials, $RuO_2{\cdot}xH_2O$ nanoparticles, are uniformly dispersed on the surface and serve as highly active components in fast redox reactions, which enormously improves the pseudocapacitance. At the same time, the fact that the surface of $RuO_2{\cdot}xH_2O$ is exposed is beneficial for the transportation and exchange of hydrogen ions, and it is useful in improving the rate capability during fast charging and discharging processes. Moreover, metallic conductivity for both the carbon shell and the RuO_2 layer is favorable for the construction of an "expressway" for electron transfer under the aid of self-assembly of the uniform nanospheres into densely stacked networks.[22–23] Furthermore, the mesoporosity of the carbon shell and the hollow structure in these nanospheres will result in efficient diffusion of the electrolyte into every corner of the sample, and many defects originating from template-assisted synthesis will probably lead to hydrophilic surface areas,[24] both of which promote the charge storage performance. Cyclic voltammetry (CV) measurements indicate that high specific capacitance together with good rate capability are highly characteristic of the obtained hierarchical architecture, implying the potential application of the product in electrochemical energy storage.

The overall synthesis is based on a template-assisted strategy as shown in Scheme 1. Searching for an appropriate approach to make hollow carbon nanospheres is the first step.

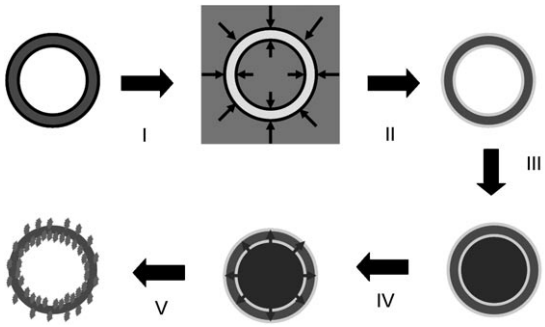

Scheme 1. Schematic illustration for the total synthetic strategy of RuO_2/C/RuO_2 sandwiched and hierarchical architecture. Carbon hollow nanospheres absorb $RuCl_3$ from solution (steps I and II) and the absorbed $RuCl_3$ reacts with NaOH when nanospheres are impregnated in the basic solution (steps III and IV) to form $RuO_2{\cdot}xH_2O$ nanoparticles (step V).

So far, several preparation methods have been reported in which nanospheres of various materials with hollow structures and mesoporous shells have been developed.[25–29] Next, some kind of carbon precursor should be deposited or coated onto the surface area of the mesoporous nanospheres, which are then transformed into carbon hollow nanospheres with a mesoporous shell once necessary processes of calcination and dissolution have been carefully completed. Among these methods, the SnO_2-supported preparation route has been finally accepted owing to its simplicity, reliability, and high reproducibility (see the Supporting Information). In general, the obtained carbon hollow nanospheres demonstrate high surface areas and a great amount of defects, qualities that are desirable for their subsequent homogeneous dispersion into $RuCl_3$ aqueous solution (0.025 M) under the aid of strong ultrasonication for 10 min (Scheme 1, step I). Upon drying at 95 °C overnight, these carbon nanospheres serve as spongelike supporters to absorb Ru^{3+} cations thoroughly, relying on the large outer and inner surface areas (Scheme 1, step II). Afterwards, a certain volume of NaOH aqueous solution (3 M) is incorporated into these nanospheres with the assistance of capillary force (Scheme 1, step III). Meanwhile, the NaOH solution will partially redissolve the absorbed Ru^{3+} cations. When the temperature is increased to 60 °C from room temperature, the volumetric expansion of the incorporated NaOH/$RuCl_3$ solution causes some of the solution to be expelled out of the pores and enables the outer layers of nanospheres

to be covered by the mixed solution (Scheme 1, step IV). At the same time, a higher temperature can accelerate the reaction rate between OH^- and Ru^{3+} species, and as a consequence, $RuO_2{\cdot}xH_2O$ nanoparticles have been generated in situ around both the outer and inner surface areas, resulting in a concentric and sandwiched architecture with characteristics of three-fold layers of $RuO_2/C/RuO_2$ (Scheme 1, step V).

The structure of the carbon capsules and their synthetic procedure was investigated in detail by using transmission electron microscopy (TEM) as presented in Figure 1. As shown in Figure 1a, uniform and spherical products were clearly detected, and more importantly, the hollow nature of these products (from SnO_2 hollow nanospheres derived from the Ostwald ripening process) indicated that they were highly qualified to be employed as templates to synthesize other functional systems.[29] From the gradually magnified TEM images (as demonstrated in sequence from Figure 1b–d), it could be distinctly detected that by undergoing the subsequent stepwise treatments of encapsulation of glucose (see the Supporting Information), carbonization, acidic/alkaline dissolution, and drying processes, carbon hollow nanospheres could be formed (Figure 1b and 1c). These carbon nanospheres presented a well-graphitized shell (Figure 1d) with regular spherical spaces inside, which were mesoporous. All of the above characteristics would provide optimal conditions for their subsequent functionalization.

The final products ideally duplicated the morphology of the precursors, as revealed in Figure 2a and b, the scanning electron microscopy (SEM) images. The low-magnification SEM image Figure 2a illustrates some monodisperse nanospheres with an almost uniform diameter of 300–400 nm and its corresponding enlarged SEM image shown in Figure 2b illustrates that some tiny particles were evenly distributed on the outer surfaces of these nanospheres. In Figure 2c, the low-magnification TEM image presents some double-layered nanospheres under high-energy electron beam irradiation (200 kV), which are totally different from their carbon nanosphere precursors (Figure 1b–d). This implies that some $RuO_2{\cdot}xH_2O$ had been successfully deposited onto the double layers of these carbon spheres, because elements with heavier atomic masses normally exhibit a better capability for E-beam dispersion and display much darker domains in TEM images. Additionally, energy-dispersive X-ray spectroscopy (EDX) also reflected the existence of elemental Ru in our samples (see the Supporting Information) and high-resolution TEM (HRTEM) was used to characterize them. Figure 2d and e presents a very clear structural description. A thin film consisting of $RuO_2{\cdot}xH_2O$ nanoparticles of around 2 nm in diameter surrounded the outside and formed the outermost layer of the overall sandwiched structure (Figure 2d and e). Slightly larger crystals of up to 10 nm were universally spread throughout the inner surface areas, indicating the formation of the second layer of $RuO_2{\cdot}xH_2O$. Owing to capillary forces, the mixed solution of $RuCl_3$ and NaOH were preferentially extracted into the inner vacancies in the carbon nanospheres. As a result, most of the precursors predominantly remain inside the carbon nanospheres, and through in situ reactions, $RuO_2{\cdot}xH_2O$ could aggregate and grow into larger crystals compared with those outside (Figure 2d and e). Finally, the section between the two $RuO_2{\cdot}xH_2O$ layers was destined to be a carbon shell layer.

This hierarchical structure is composed of $RuO_2{\cdot}xH_2O$ (the most promising electrode material for pseudocapacitance) and mesoporous carbon (the conventionally used economical electrode material for ECs), and so the combi-

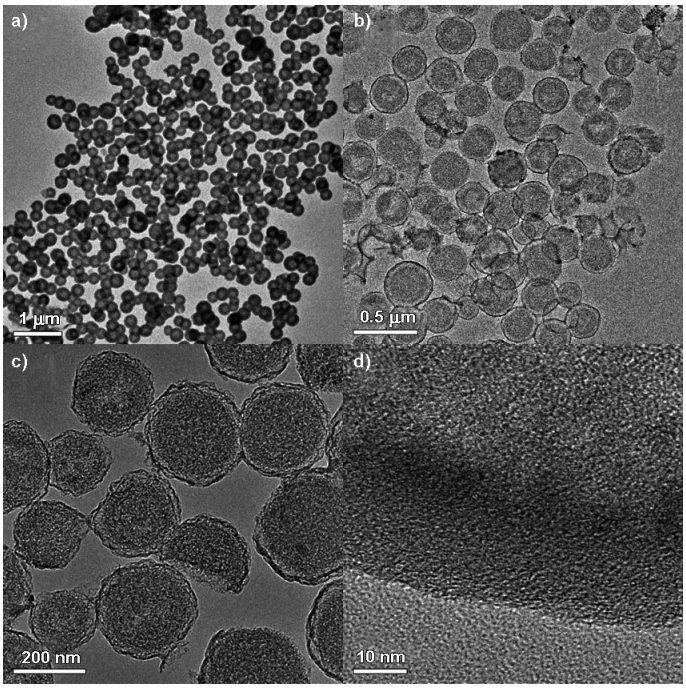

Figure 1. a) TEM images of SnO_2 hollow nanospheres, b)–d) Gradually magnified TEM images of carbon hollow nanospheres.

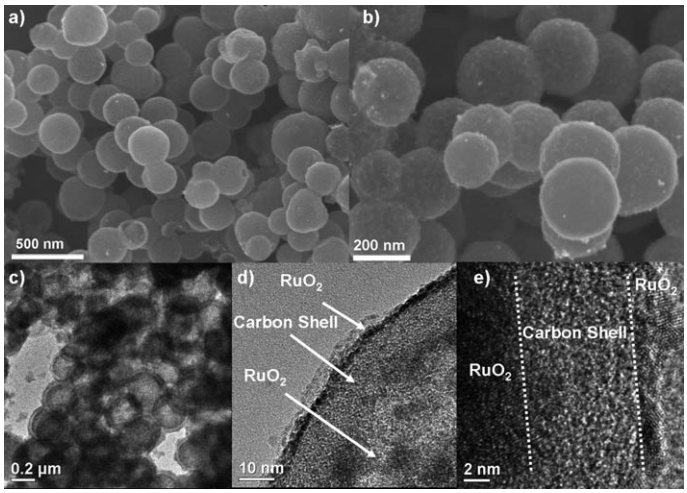

Figure 2. SEM images of $RuO_2/C/RuO_2$ sandwiched and hierarchical nanospheres (a and b) and their typical TEM image (c) together with the corresponding locally magnified HRTEM images (d and e).

nation may offer all the possible advantages from both components. Typical nitrogen adsorption–desorption isotherm and pore-size distribution curves for the samples are shown in Figure 3a and its inset, respectively. The extremely high surface area of 756.4 $m^2 g^{-1}$ and pore size centered at 2.7 nm demonstrate that the samples could be expected to possess excellent double-layer capacitance. By means of CV measurements, the electrochemical properties of the hierarchical samples could be investigated. Prior to the measurement, annealing of the samples at 200 °C for 2 h was necessary because a balance between electron and proton transfer for the redox transitions of oxyruthenium species among various oxidation states must be achieved, which will subsequently promote the pseudocapacitance of $RuO_2 \cdot xH_2O$.[30] Figure 3b shows the CV curves collected under low scan rates ranging from 5 to 200 mV s^{-1}. The nearly rectangular profiles reveal that the samples exhibited excellent performance for the application of ECs, because not only is smooth and rapid charge–discharge highly expected, but also a stable power supply can be guaranteed from the rectangular profiles.[2,24] The broad peak located at potentials (E vs. Ag/AgCl) of around 0.38 and 0.27 V implies that redox reactions occurred during the scan period, which originated from either redox transitions among various oxidation states of $RuO_2 \cdot xH_2O$[18] or the oxygen-rich groups developed from the templated synthesis.[24] The maximum specific capacitance was above 550 F g^{-1} when the scan rate was decreased to 5 mV s^{-1}, and with the scan rate increasing gradually, the specific capacitance was accordingly reduced (Figure 3b). Such a result can be reasonably understood based on the mechanisms of charge storage. Up to now two mechanisms of charge storage have been raised. The first one is dependent on the double-layer capacitive behavior, and the second one relies on the redox reactions of pseudocapacitance. However, whichever is selected, two factors, including penetration or diffusion of the electrolyte into the inner structures of the electrode materials and charge exchange/separation at the interface between the electrolyte and the electrode materials, must be taken into consideration owing to their effect on the rate-determining steps.[2,7,12,18] Commonly, the electrolyte diffusion or charge exchange rate cannot catch up with the speed of the substantially increased electrochemical reactions, as verified in the previous reports. To investigate the rate capability of the samples, even higher scan rates had been used to examine the electrochemical properties. In Figure 3c, although the scan rate was increased stepwise from 300 up to 1200 mV s^{-1}, the current density was subsequently boosted to a peak value of 600 A g^{-1}(Figure 3c). Such a high current density, which simultaneously retains an ideal specific capacitance as high as 380 F g^{-1} (Figure 3d), has scarcely been reported in the previous results, indicating that high specific capacitance can be available under very high power operation for our hierarchical samples.[21] Furthermore, electrochemical stability and cycleability had also been investigated by using a long CV scan time of up to 2000 cycles, proving the stable accessibility and retention of high specific capacitance for the samples under the tough conditions. Of course, it is inevitable that systematic conductivity would gradually deteriorate when the CV scan rate was raised (as shown in Figure 3b and c). The slopes of the originally initiated steps of charging and discharging become more vivid, as indicated by the black arrows. In our experiments, a relatively

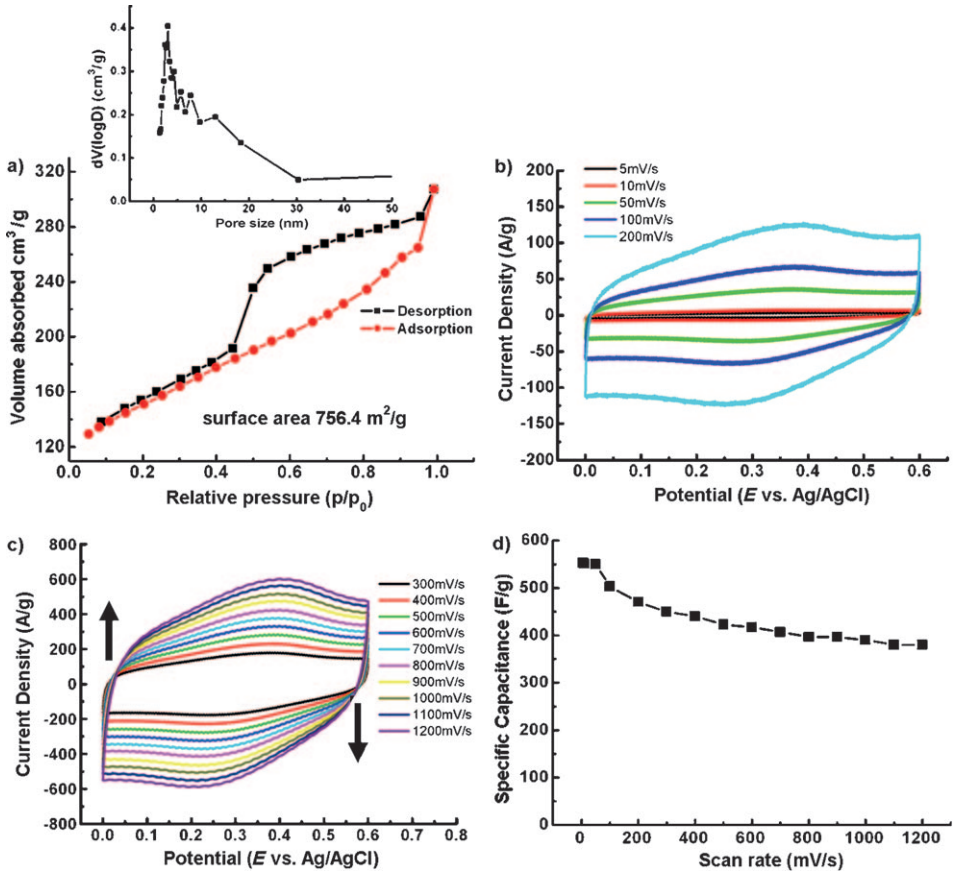

Figure 3. a) Brunauer–Emmett–Teller (BET) nitrogen absorption–desorption isotherm and the corresponding size-distribution curve (inset), b) and c) CV profiles for the RuO_2/C/RuO_2 sandwiched and hierarchical nanospheres, and d) diagram of relationship between the scan rate and the specific capacitance (illustrating a good rate capability with a high specific capacitance over a high scan rate).

narrow voltage scan range (0.6 V) had been applied to achieve the maximum specific capacitance. However, if a wider range was accepted (0.9 V), quite high specific capacitance could also be obtained (see the Supporting Information), further supporting the idea that our hierarchical samples can be operated under high power supplies.[2,7,12] Meanwhile, pure hollow carbon nanospheres were tested by using a cyclic voltammetry method to determine their capacitive performance (see the Supporting Information). Their much lower specific capacitances further verified that our hierarchical samples exhibited excellent electrochemical properties associated with their unique architecture.

The sandwiched concentric architecture obtained in our experiments represents significant innovation in the construction of functional systems, which is the exact reason why excellent capacitive performance can be achieved for our samples. As described in Scheme 2, it can be found that

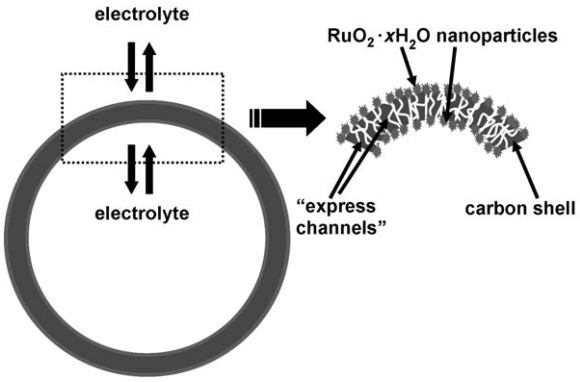

Scheme 2. Illustration of the intrinsic association between RuO_2/C/RuO_2 sandwiched and hierarchical architecture, and the excellent electrochemical performanc. Left: The structural demonstration for one hierarchical nanosphere. Right: The locally enlarged schematic image to describe the express channels in the carbon shell and the RuO_2·xH_2O nanoparticles dispersed on both the outer and inner surfaces of the carbon shell.

the electrolyte may be highly free to penetrate and diffuse between the inner and outer portions of carbon hollow nanospheres through the "express channels" within the carbon shell. Because the evolution of a hollow structure for SnO_2 nanospheres was derived from the Ostwald ripening effect, a large amount of micro- or nanochannels should exist and run through the shells.[31] Thus, these micro- or nanochannels should survive after the duplication process by using glucose as a precursor of carbonization was accomplished (Scheme 2, right). These channels, which have a diameter of 2.7 nm (inset of Figure 3a), are transfixing the carbon shell and are interconnecting the outer and inner parts of the carbon hollow nanospheres, so they can be regarded as some kind of express channels to maintain the pathway of the electrolyte. Moreover, under the aid of the express channels, the outer and inner surface areas of the carbon hollow nanospheres and the deposited RuO_2·xH_2O nanoparticles can be thoroughly utilized so that they jointly contribute to the greatly improved electrochemical performance in charge storage. Furthermore, note that both graphitized carbon and RuO_2 are perfect metallic conductive materials and that the networks assembled from them will definitely exhibit excellent conductivity, which is undoubtedly favorable for a quick response when high scan rates are applied in the CV measurements. Meanwhile, under our experimental design, RuO_2 loading can be precisely controlled below 15%, indicative of a promising candidate for practical applications in electrochemical energy storage.

In summary, we have rationally designed a sandwiched hierarchical architecture consisting of RuO_2/C/RuO_2 and have successfully employed it in the field of electrochemical energy storage. The perfect electrocapacitive performance is strongly associated with the designed smart system in which express channels play an essential part in building-up fast responsive pathways for electrolyte penetration, and more efficient utilization of all of the exposed surface areas for both mesoporous carbon shell and RuO_2·xH_2O nanoparticles. Low loading of elemental Ru and excellent specific capacitance over very high scan rates shed light on the fact that our hierarchical samples are applicable for the practical electrode materials in supercapacitors. The overall preparation strategy will provide an inspiring illustration and guidance for the design of functional systems of the future in the similar fields, especially for energy storage, for example, in supercapacitors and Li-ion batteries. The method is being extended to the synthesis of other materials such as MnO_2/C, V_2O_5/C and more results will be presented soon.

Experimental Section

Materials: All chemicals or materials were directly used without any further purification prior to usage: K_2SnO_3·$3H_2O$ (Aldrich, 99.9%), urea (Alfar Aesar, 98+%), D-(+)-glucose (Cica-Reagent, Kanto Chemical), HCl (fuming 37%, guarantee reagent (GR) for analysis, MERCK), $RuCl_3$ (Aldrich, Ru content 45–55%), NaOH (pellets, GR for analysis, MERCK), H_2SO_4 (Panreac, 96%).

Preparation of SnO_2 and carbon hollow nanospheres: Urea (0.1 M) and K_2SnO_3·$3H_2O$ (16 mM) in a mixed solvent of ethanol/water (30 mL; ethanol, 37.5 vol%) were transferred into a 45 mL Teflon-lined stainless-steel autoclave and heated at 150°C for 24 h in a preset electric oven. The autoclaves were naturally cooled to room temperature. The precipitates were harvested by centrifugation and washed by deionized water and ethanol for at least three cycles and the products were thoroughly dried at 60°C overnight in a vacuum oven.

The dried SnO_2 products (200–250 mg) were subsequently dispersed into aqueous glucose solution (30 mL, 1 M) under strong ultrasonication for 10 min and the homogeneous solution formed was heated again in a 45 mL Teflon-lined stainless-steel autoclave at 180°C for 4 h. The brown samples were centrifuged and washed with deionized water and ethanol, before being tried in a vacuum oven at 100°C for 3 h. After finishing the calcinations of these dried samples at 700°C for 200 min in an atmosphere of Ar, the final products were evenly dispersed in HCl (3 M) to remove the residual SnO_2 and the reduced metallic Sn. In the last cycle, NaOH (3 M) was used to functionalize the surfaces of carbon nanospheres and the samples were dried at 100°C overnight in a vacuum oven.

Synthesis of RuO_2/C/RuO_2 sandwiched hierarchical architectures: An aqueous solution of $RuCl_3$ (1 mL, 0.025 M) was extracted by using a micropipette and was dropped onto hollow carbon nanospheres (20 mg),

and the black sol-gel was dried at 95 °C in a vacuum oven until water was completely removed from the products. Then, an aqueous solution NaOH (0.16–0.25 mL, 3 M) was introduced into the above products dropwise, and the mixture was left to slowly react at 60 °C for 30 min. Finally, the reacted samples were washed and purified by washing three times with deionized water and then once with ethanol in a centrifuge. The same procedure can be repeated several times to increase the absorbed quantity of Ru.

Characterization of the samples: SEM (FEI, 5 kV, coupled with energy dispersive X-ray spectroscopy), TEM (Philips, Tecnai, F20, 200 kV), and BET surface-area measurements (Quantachrome Autosorb-6B surface area & pore size analyzer) were applied to characterize the obtained samples.

Electrochemical testing: The samples (2–10 mg) were mixed with the solvent mixture (2–4 mL; DI H2O/2-propenol/Nafion, 80:15:5 % v/v). Then the mixture was strongly stirred for 3 days resulting in a homogeneous solution. Some of this mixture (10 μL) was extracted by using a micropipette and was dropped onto the graphite electrode to serve as a working electrode after being naturally dried in air and subsequently thermally treated at 60 °C for 1 h. The electrochemical properties of the sample were tested by using an Autolab potentiostat (model of AUT71740) and a three-electrode cell. Pt foil was used as the counter electrode, Ag/AgCl as the reference electrode, and an aqueous solution of H_2SO_4 (0.5 M) as the electrolyte.

Acknowledgements

This work was financially supported by Intelligent Energy Distribution Systems (IEDS) of the Agency for Science, Technology, and Research (ASTAR), Singapore. Dr. Yu Wang is sincerely grateful for the valuable discussion with Dr. Huijuan Zhang from Nanyang Technological University (NTU).

Keywords: carbon · electrochemistry · energy transfer · nanomaterials · ruthenium

[1] M. Winter, R. J. Brodd, *Chem. Rev.* **2004**, *104*, 4245–4269.
[2] P. Simon, Y. Gogotsi, *Nat. Mater.* **2008**, *7*, 845–854.
[3] G. K. Mor, O. K. Varghese, M. Paulose, K. Shankar, C. A. Grimes, *Solar Energy Materials Sol. Cells* **2006**, *90*, 2011–2075.
[4] Z. L. Wang, *Adv. Funct. Mater.* **2008**, *18*, 3553–3567.
[5] H. Li, Z. X. Wang, L. Q. Chen, X. J. Huang, *Adv. Mater.* **2009**, *21*, 4593–4607.
[6] M. Gyu Kim, J. Cho, *Adv. Funct. Mater.* **2009**, *19*, 1497–1514.
[7] A. Burke, *J. Power Sources* **2000**, *91*, 37–50.
[8] E. Frackowiak, *J. Braz. Chem. Soc.* **2006**, *17*, 1074–1082.
[9] Y. G. Guo, J. S. Hu, L. J. Wan, *Adv. Mater.* **2008**, *20*, 2878–2887.
[10] J. R. Miller, P. Simon, *Science* **2008**, *321*, 651–652.
[11] B. E. Conway, *Electrochemical Supercapacitors: Scientific fundamental and Technological Applications*, Kluwer, Drodrecht, **1999**.
[12] R. Kötz, M. Carlen, *Electrochim. Acta* **2000**, *45*, 2483–2498.
[13] A. G. Pandolfo, A. F. Hollenkamp, *J. Power Sources* **2006**, *157*, 11–27.
[14] J. Chmiola, G. Yushin, Y. Gogotsi, C. Portet, P. Simon, P. L. Taberna, *Science* **2006**, *313*, 1760–1763.
[15] N. L. Wu, *Mater. Chem. Phys.* **2002**, *75*, 6–11.
[16] T. Brousse, *J. Electrochem. Soc.* **2006**, *153*, A2171–A2180.
[17] A. Rudge, I. Raistrick, S. Gottesfeld, J. P. Ferraris, *J. Power Sources* **1994**, *47*, 89–107.
[18] C. C. Hu, K. H. Chang, M. C. Lin, Y. T. Wu, *Nano Lett.* **2006**, *6*, 2690–2695.
[19] J. M. Miller, B, Dunn, T. D. Tran, R. W. Pekala, *J. Electrochem. Soc.* **1997**, *144*, L309–L311.
[20] M. Min, K. Machida, J. H. Jang, K. Naoi, *J. Electrochem. Soc.* **2006**, *153*, A334–A338.
[21] H. Zhang, G. P. Cao, Z. Y. Wang, Y. S. Yang, Z. J. Shi, Z. N. Gu, *Nano Lett.* **2008**, *8*, 2664–2668.
[22] Y. G. Guo, Y. S. Hu, W. Sigle, J. Maier, *Adv. Mater.* **2007**, *19*, 2087–2091.
[23] X. W. Lou, C. M. Li, L. A. Archer, *Adv. Mater.* **2009**, *21*, 2536–2539.
[24] H. Pan, C. K. Poh, Y. P. Feng, J. Y. Lin, *Chem. Mater.* **2007**, *19*, 6120–6125.
[25] T. R. Zhang, J. P. Ge, Y. X. Hu, Q. Zhang, S. Aloni, Y. D. Yin, *Angew. Chem.* **2008**, *120*, 5890–5895; *Angew. Chem. Int. Ed.* **2008**, *47*, 5806–5811.
[26] J. Liu, H. Xia, D. F. Xue, L. Lu, *J. Am. Chem. Soc.* **2009**, *131*, 12086–12087.
[27] J. Li, H. C. Zeng, *J. Am. Chem. Soc.* **2007**, *129*, 15839–15847.
[28] S. B. Yoon, K. Sohn, J. Y. Kim, C. H. Shin, J. S. Yu, T. Hyeon, *Adv. Mater.* **2002**, *14*, 19–21.
[29] X. W. Lou, C. L. Yuan, L. A. Archer, *Small* **2007**, *3*, 261–265.
[30] W. Dmowski, T. Egami, K. E. Swider-Lyons, C. T. Love, D. R. Rolison, *J. Phys. Chem. B* **2002**, *106*, 12677.
[31] X. W. Lou, D. Deng, J. Y. Lee, L. A. Archer, *Chem. Mater.* **2008**, *20*, 6562–6566.

Received: November 16, 2009
Published online: February 28, 2010

